J Mater Sci (2007) 42:2934–2943
DOI 10.1007/s10853-006-0565-y

ADVANCES IN GEOPOLYMER SCIENCE & TECHNOLOGY

Alkali activation of metakaolins: parameters affecting mechanical, structural and microstructural properties

M. Luz Granizo · M. T. Blanco-Varela ·
S. Martínez-Ramírez

Received: 20 September 2005 / Accepted: 13 June 2006 / Published online: 23 January 2007

Abstract The composition, structure and properties of the reaction product resulting from the alkali activation of metakaolin (MK) are directly impacted by the specific surface and composition of the initial kaolin and the type, concentration and relative amount of alkali activator used. This study aimed to analyze the effect of these parameters on the flexural strength, degree of reaction, porosity and chemical and mineralogical composition of alkali-activated metakaolin pastes. Two types of metakaolin with different specific surfaces were activated under hydrothermal conditions (85 °C, 2 h) using solutions consisting of waterglass and Na(OH) as activators (Na concentrations = 6, 8, 10, 12, 15, 18, 20 M) and two metakaolin/solution ratios. Regression analysis was used to quantify the effect of the parameters tested (activator concentration and MK/solution ratio) on flexural strength. Mathematical models were likewise built to relate the degree of reaction and amount of sodium fixed in the polymer structure to the synthesis parameters. According to ^{29}Si and ^{27}Al MAS NMR, XRD, FTIR, DTA/TG data and chemical analysis, the material obtained by activating two MKs with waterglass plus NaOH was an amorphous hydrated sodium aluminosilicate in which a Q^4 Si (3Al) type three-dimensional structure predominated, i.e., a structure where three Al atoms are connected to SiO_4 tetrahedra. The alkaline ions in the structure maintain the electrical balance. The general formula obtained for this inorganic polymer was $Na_2O{\cdot}3SiO_2{\cdot}Al_2O_3{\cdot}3H_2O$.

Introduction

The alkali activation of metakaolins yields strong and durable cementitious materials that harden at temperatures of under 100 °C [1–3]. The composition, structure and properties of the reaction product obtained in the alkali activation of metakaolin are directly impacted by the specific surface and composition of the initial kaolin and the type, concentration and relative amount of alkali activator used [3–7].

The product of metakaolin activation with NaOH solutions is an amorphous cementitious material [3, 6–8]. It has been concluded from FTIR, ^{27}Al, ^{29}Si MAS NMR and ^{23}Na MAS NMR [1–6] studies that its three-dimensional structure is a network [Q^4(Al)] consisting in alternating SiO_4 and AlO_4 tetrahedra linked by shared O atoms. The alkali cations in the structure balance the negative charge of the tetrahedrally coordinated Al^{3+} ion. Its composition corresponds to the general formula: $2SiO_2{\cdot}Al_2O_3{\cdot}Na_2O{\cdot}2H_2O$ [7].

In the present study, two types of metakaolin with different specific surfaces were activated under hydrothermal conditions (85 °C, 2 h) using solutions consisting of waterglass and Na(OH) as activators (Na concentrations 6, 8, 10, 12, 15, 18, 20 M) and two metakaolin/solution ratios. The aim was to analyze the effect of these parameters on the flexural strength, degree of reaction, porosity and chemical

M. L. Granizo
SIKA S.A., Ctra Fuencarral 72, 28108 Alcobendas, Madrid, Spain

M. T. Blanco-Varela (✉) · S. Martínez-Ramírez
Instituto de Ciencias de la Construcción Eduardo Torroja (CSIC), c/ Serrano Galvache 4, 28033 Madrid, Spain
e-mail: blancomt@ietcc.csic.es

and mineralogical composition of alkali-activated metakaolin pastes.

Experimental

Two kaolins—from Guadalajara (K1) and Tudela (K2), Spain—were heated at 750 °C for 24 h to obtain their respective metakaolins. The chemical analysis of these compounds is given in Table 1. K1 and K2 contain 12.4 and 7%wt, respectively, of quartz as the secondary mineral [8]. The BET specific surface was MK1 = 7.7 m^2/g and MK2 = 6.7 m^2/g [4].

Specimens were made from mixes containing two types of metakaolin (MK1 and MK2) and different solutions of waterglass and NaOH, at variable MK/liquid ratios. These 10 × 10 × 60 mm specimens were cured in sealed boxes, for 2 h at 85 ± 2 °C and 90% RH. The activators were prepared by mixing solid NaOH and waterglass to obtain six solutions with the following Na concentrations: 6, 8, 10, 12, 15, 18 and 20 M. Since the rheological behaviour of MK1 and MK2 differs substantially (due primarily to fineness differences), 50 or 60 ml of activating solution were mixed with 70 g of compound to make the MK1 specimens, whereas 30 or 35 ml of activating solution were used per 70 g of MK to make the MK2 specimens. The SiO_2/NaO_2 molar ratio in the waterglass used was 3.41; the density was 1.35 g/ml and the total solids, 34.40%wt (Crosfield Limited Crystal C70).

Table 1 Chemical analysis of the two kaolins (%wt)

	SiO_2	Al_2O_3	Fe_2O_3	MgO	CaO	LOI
Kaolin 1	49.8	36.3	0.6	0.2	0.0	12.6
Kaolin 2	47	36.0	0.5	0.0	0.8	11.7

LOI lost on ignition

Of the 12 prisms made and cured for each composition, 11 were used to determine flexural strength and one to find porosity with a Micromeritics 9320 V2.02 mercury porosimeter. Table 2 gives the composition of the specimens.

The pastes obtained were characterized by differential thermal analysis and thermogravimetry (DTA/TG), X-ray diffraction (XRD), Fourier transform infrared spectroscopy (FTIR) and nuclear magnetic resonance (samples I, K, B, D) (^{29}Si MAS NMR, ^1H-^{29}Si CP MAS NMR, ^{27}Al MAS NMR and ^{23}Na MAS NMR).

Table 2 Dissolution volume and NaOH concentration in the solution by 70 g of metakolin. Porosity, flexural strength, soluble and fixed Na and IR of the specimens (elaborated with pastes cured 2h at 85°C)

Label	V (ml)	Na (M)	Na_2O/SiO_2	H_2O/Na_2O	SiO_2/Al_2O_3	Flexur. str. (MPa)	IR (%wt)	Porosity (%vol)	%Na $_2$O soluble (DR)[a]	%Na $_2$O fixed (DR)[a]
MK2										
A	30	6	0.11	15.57	2.88	0	77.05	26.0	3.67	3.02
B	30	8	0.15	12.03	2.88	11.8 ± 0.2	52.97	34.4	1.71	6.93
C	30	10	0.18	9.87	2.88	13.0. ± 0.3	45.19	30.0	2.44	8.09
D	30	12	0.22	8.42	2.88	13.9 ± 0.2	38.56	20.7	2.21	10.12
E	30	15	0.27	6.96	2.88	9.5 ± 0.2	29.42	17.2	2.93	11.98
F	30	18	0.32	5.98	2.88	8.9 ± 0.3	27.57	25.6	4.47	12.87
G	30	20	0.36	5.49	2.88	8.57 ± 0.2	23.56	27.1	5.56	13.32
A′	35	6	0.12	15.57	2.98	0	72.17	37.7	5.36	2.19
B′	35	8	0.16	12.03	2.98	10.5 ± 0.2	48.05	37.1	2.34	7.41
C′	35	10	0.20	9.87	2.98	12.8 ± 0.1	39.97	29.4	2.40	9.42
L	35	12	0.24	8.42	2.98	12.9 ± 0.3	41.25	30.9	2.26	11.56
E′	35	15	0.30	6.96	2.98	9.1 ± 0.2	24.68	19.7	5.51	11.15
F′	35	18	0.36	5.98	2.98	8.0 ± 0.3	21.26	27.0	5.13	14.17
G′	35	20	0.40	5.49	2.98	6.3 ± 0.2	21.77	31.2	6.76	14.21
MK1										
H′	50	6	0.16	12.57	3.44	1.6 ± 0.3	62.83	55.8	5.19	4.71
I′	50	8	0.21	12.03	3.44	8.2 ± 0.2	32.25	44.9	1.88	10.80
J′	50	10	0.26	9.87	3.44	7.5 ± 0.3	23.35	32.3	2.44	12.84
M	50	12	0.31	8.42	3.44	10.2 ± 0.3	17.36	24.9	2.85	14.88
O	50	15	0.39	6.96	3.44	7.5 ± 0.2	12.23	29.6	6.10	15.07
H	60	6	0.18	15.58	3.66	0	61.30	54.9	6.27	4.94
I	60	8	0.24	12.03	3.66	8.1 ± 0.1	23.81	51.8	2.61	11.69
J	60	10	0.29	9.88	3.66	8.0 ± 0.3	15.60	43.6	2.86	14.32
K	60	12	0.35	8.42	3.66	8.8 ± 0.2	14.12	39.8	5.48	14.40
N	60	15	0.44	6.96	3.66	5.7 ± 0.2	10.34	31.4	9.41	14.19

Flexural strength, porosity and IR of the specimens (elaborated with pastes cured 2h at 85 °C). $\%Na_2O$ soluble and fixed

[a] (DR) = percentage of sodium in terms of dry residue, where DR = (%MK + $\%Na_2O$ + $\%SiO_2$)

The DTA/TG studies were conducted with a Netzsch ATA 409 simultaneous thermal analyzer. The heating rate was 4 °C/min, the sample mass was 200 mg and the maximum temperature 1,000 °C.

The X-ray diffraction patterns of the powdered samples were recorded on a Philips PW 1730 diffractometer using CuKα radiation. The tests were run in a 2θ range of 5–60° at a scanning rate of 2°/min, with a divergence slit of 1°, an anti-scatter slit of 1° and a receiving slit of 0.01 mm.

The FTIR spectra were recorded on an ATI Mattson FTIR-TM series spectrometer. Specimens were prepared by mixing 1 mg of the sample in 300 mg of KBr. The spectral analysis was performed in the range 4,000–400 cm^{-1}, with a spectral resolution of 4 cm^{-1}.

Solid-state ^{29}Si, ^{27}Al and ^{23}Na NMR spectra were obtained with a Bruker MLS-400 spectrophotometer working at 79.49 and 104.26 MHz, respectively. ^{29}Si and ^{27} Al MAS NMR spectra were obtained after $\pi/2$ pulse excitations (4 μs) and 5 s of recycling delays. Spectra were recorded with MAS techniques, with sample spinning rates of 4 and 12 kHz. The number of scans was 800 and 200, respectively for ^{29}Si and ^{27}Al spectra. Baseline distortions were eliminated after correction of dead time effects. ^{29}Si and ^{27}Al chemical shifts were reported with respect to tetramethylsilane (TMS) and 1M $AlCl_3{\cdot}6H_2O$ solutions, respectively.

The insoluble residue (IR) in dilute acid was determined for each paste using a procedure that dissolves the reaction products without attacking the unreacted metakaolin in the sample [3]. Loss on ignition at 1,000 °C and the soluble sodium in cured pastes were determined with a methodology described elsewhere [3].

Since the degree of reaction in the activated pastes is under 100%, they contain a mix of reaction product (alkaline polymer) and reagents (MK and NaOH) in their composition. Due to this, the composition of the polymer obtained does not concur with the composition of the initial reagents. Consequently, samples M, F and D were analyzed using the methodology described in a previous paper [7] to determine the chemical composition of the alkaline polymer. For this same reason, total sodium, aluminium and silicon were likewise determined for these samples, as well as for the solid residues remaining after the samples were attacked with dilute acid [7].

Results

The two kaolins and their respective metakaolins were fully characterized (chemical and mineralogical composition, thermal behaviour, specific surface, particle size distribution, and so on) in previous studies [4, 8]. MK1 and MK2 behaviour when activated with different concentrations of NaOH has also been reported elsewhere [3, 7]. Table 2 shows the composition of the metakaolin pastes activated with different waterglass + NaOH solutions, along with specimen flexural strength, porosity, the insoluble residue in dilute HCl and %Na_2O fixed and soluble.

The XRD traces for the two metakaolins and sample M are reproduced in Fig. 1. The only crystalline phase in MK1 is quartz, while the diffractogram for MK2 shows low intensity reflections attributed to dehydroxylated pyrophyllite and anatase [9, 10]. The diffractograms for all the MK1 pastes contain quartz crystal reflections and a halo at $2\theta = 30°$, indicative of an essentially amorphous compound. The position of this halo, at larger angles than in the patterns for the initial MK1, is characteristic of the alkaline polymers obtained [5, 11]. The additional diffraction lines visible in the XRD patterns for samples O and N at 2θ = 5.88°, 9.84°, 11.40°, 15.18°, 19.74°, 23.16°, 28.98°, 30.72°, 40.72° are attributed to the crystallization of a faujasite-type sodium aluminosilicate.

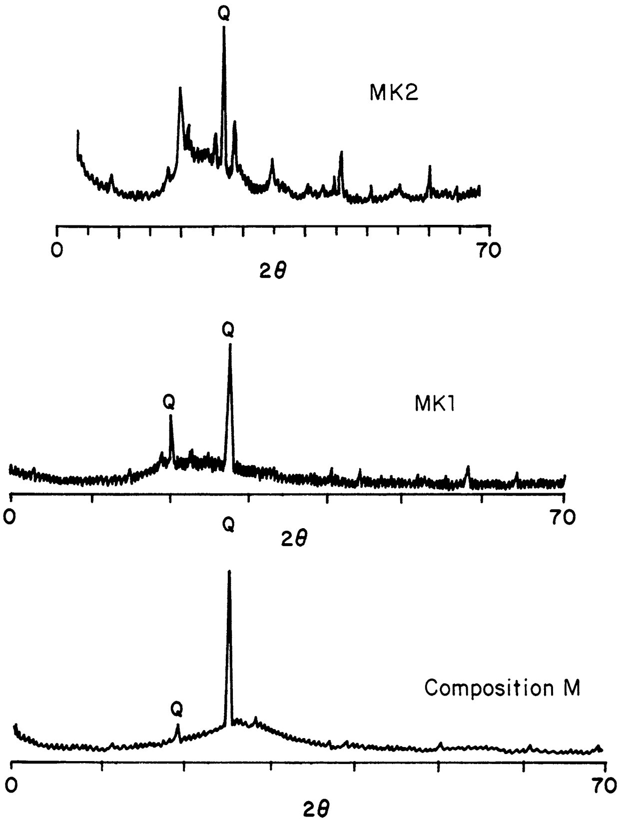

Fig. 1 XRD patterns of MK1, MK2 and Composition M

The diffractograms for the MK2 pastes, with a halo at $2\theta = 30°$, are likewise indicative of amorphous materials; reflections of the quartz, pyrophyllite and anatase from the unreacted metakaolin are also visible; tiny faujasite reflections can be seen on the patterns for pastes E and E′, and samples F, G, F′ and G′, in turn, contain sodalite reflections. Hence, slight zeolite crystallization is observed in the samples of the two metakaolin pastes activated with alkaline solutions in which the Na concentration is 15 M or higher. This finding concurs with results reported by Rahier et al. [12], who obtained sodium aluminosilicates that were not wholly amorphous in sodium silicate-activated metakaolin samples having a SiO_2/Na_2O molar ratio of under 0.8.

Figure 2 shows the FTIR spectra for MK1, MK2 and some of the pastes obtained. The MK1 spectrum contains wide bands at 460, 1,090 and 1,150 cm^{-1}, indicative of the Si–O vibrations in the SiO_4 molecule. These signals are observed at frequencies higher than assigned to these compounds in the literature [13]. The band appearing at 800 cm^{-1} corresponds to the Al–O vibration in the tetrahedrally coordinated AlO_4 molecule [8, 11].

The spectra for the activated MK1 pastes (Fig. 2) show a band at 445 cm^{-1} and a very wide band at 584 cm^{-1}; the band at approximately 700 cm^{-1} is characteristic of the amorphous polymer formed [11]. Other findings include the disappearance of the band at 800 cm^{-1}, attributed to the condensed AlO_4 in the metakaolin, and the shift in the Si–O–Al vibration band from approximately 1,090 to 987 cm^{-1} [11, 13, 14]. When 15-M activator is used, a group of bands corresponding to the zeolite that crystallizes at this concentration is observed to develop at around 619–662 cm^{-1} [11].

The FTIR spectrum for MK2 contains absorption bands corresponding to Si–O vibrations (486, 1,048, 1,085 and 1,136 cm^{-1}) due to metakaolin and anhydrous pyrophyllite [11, 15] and to Al–O (at 802 cm^{-1}) vibrations due to metakaolin. In addition, a sharp intense signal attributed to dehyroxylated pyrophillite is visible at around 566 cm^{-1}, assigned to Si–O–Al stretching vibrations [15]. The spectra for the MK2 activated pastes contain bands in the 420–490 cm^{-1} range that correspond to the dehydroxylated pyrophyllite present in the initial metakaolin. The intense band at 486 cm^{-1} is more intense in the MK2 spectrum than

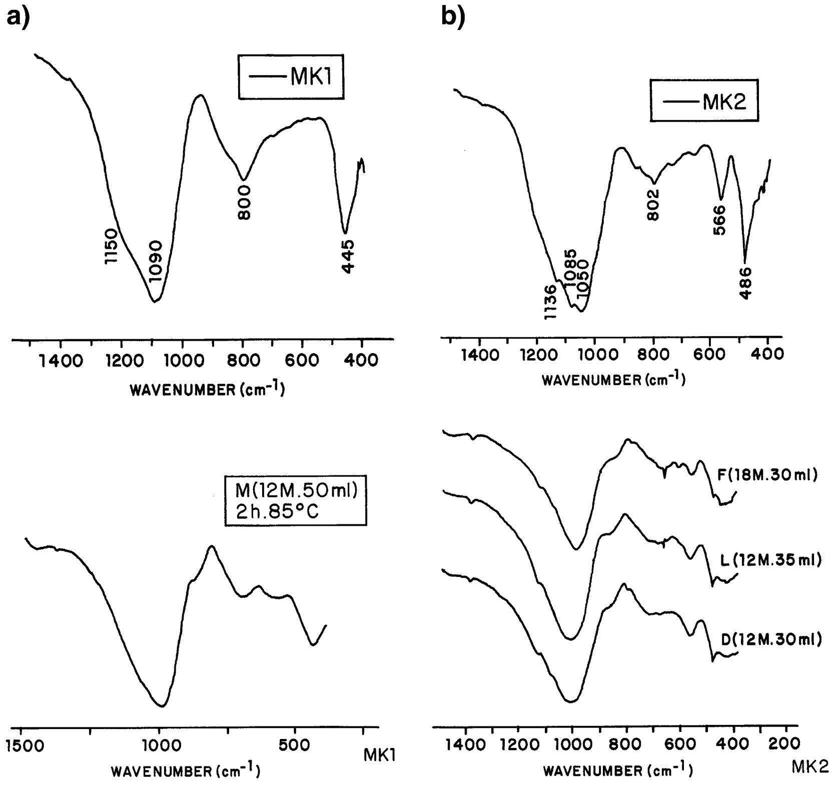

Fig. 2 (**a**) FTIR spectra for MK1 and sample M, (**b**) FTIR spectra of MK2 and F, L and D samples

Table 3 Chemical shift in the main signals on the ^{27}Al, ^{29}Si, ^{23}Na MAS NMR and [^{1}H]-^{29}Si CP MAS NMR spectra for the samples studied

MK	Sample	^{27}Al δ (ppm)	^{29}Si δ (ppm)	^{1}H^{29}Si δ (ppm)	^{23}Na δ (ppm)
	MK2	59.5			
		38.7	–107.8		
		2.6	–101.4		
MK2	B		–106.7		
		57.2	–101.3	–87.1	–9.9
		2.6	–90.1		
MK2	D		–101.2		
		57.7	–89.8	–87.1	–9.4
		2.6	–86.6		
	MK1	55.3			
		29.7	–108.0		
		2.5			
MK1	I	57.4	–90.8		–9.4
MK1	K	57.4	–88.4	–86.5	–9.0

in their activated pastes spectra [11]. The band at 566 cm^{-1} attributed to the pyrophyllite in the initial metakaolin is still visible, although less intense. A new band characteristic of the reaction product formed can be seen developing at 700 cm^{-1} [11]. The bands at around 800 cm^{-1} on the spectra for the initial metakaolin corresponding to Al(IV)–O vibrations are also observed to disappear, while the Si–O vibration band at 1,050–1,136 cm^{-1} shifts to lower frequencies (1,000 cm^{-1}) [13, 14]. The infrared spectrum for these compositions shows no substantial variation when the amount of liquid is increased. At higher Na concentrations, the band at approximately 1,000 cm^{-1} shifts to lower frequencies (990 cm^{-1}). This shift is greater than observed by Barbosa et al. [5] and confirms the results published by other authors [13], who reported an increase in the shift in the said band with decreasing SiO_2/Na_2O ratios in the activating solution.

Table 3 shows the chemical shifts corresponding to the most intense bands on the ^{27}Al, ^{29}Si MAS NMR, ^{29}Si MAS NMR, [^{1}H]-^{29}Si CP MAS NMR and ^{23}Na MAS NMR spectra for some of the pastes.

The ^{29}Si NMR spectrum for MK2, shown in Fig. 3a, has a very wide and asymmetric band with two intense signals at –107.8 ppm (Q^{4} (0Al)) and at –101.4 ppm (Q^{4} (1Al)), respectively attributed to the tetrahedral Si in the metakaolin and the pyrophyllite present in the sample [16, 17]. A wide signal appears at –91.0 ppm in the sample activated with an 8 M solution (Sample B); although less intense than in the initial spectrum, the signals for the 53% unreacted MK2 in the sample are also visible. The width of the sample is indicative of the existence of different environments for Si [5, 6, 16].

As expected, the unreacted MK2 bands disappear from the ^{1}H-^{29}Si CP MAS NMR spectrum for the activated sample; the signal appearing here at –87.1 ppm is narrower than the analogous bands observed in the spectra discussed above. When the activator concentration is increased (Sample D), the spectra are similar to those described above, although the signals attributed to unreacted MK (38%) are less intense in the spectrum recorded in single pulse mode.

The initial spectrum for MK1, reproduced in Fig. 3b, also has a very wide and asymmetric band peaking at –108 ppm (Q^{4} (0Al)) [16, 17], whose intensity declines substantially when the samples are activated with 8 and 12 M solutions (IR = 23.8 and 14.1%wt, respectively). This gives rise to a wide signal that peaks at –90.8 ppm for Sample I and –88.4 ppm for Sample K, where a

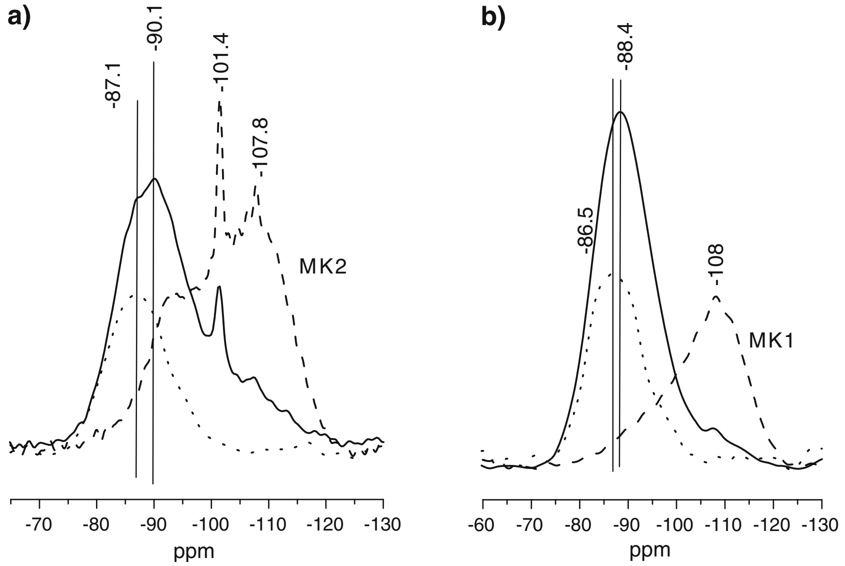

Fig. 3 (**a**) ^{29}Si MAS NMR of MK2 (*dash*) and sample D recorded in single pulse (*solid*) and CP (*dot*) mode. (**b**) ^{29}Si MAS NMR of MK1 (*dash*) and sample K recorded in single pulse (*solid*) and CP (*dot*) mode

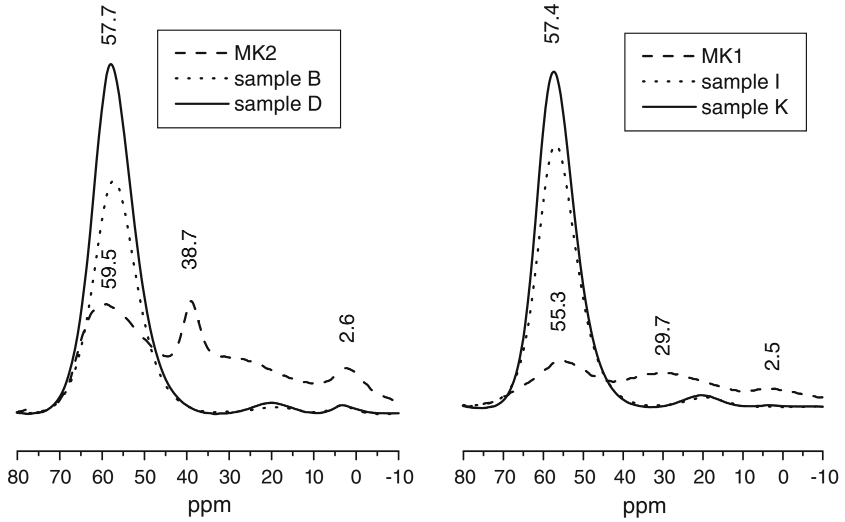

Fig. 4 *Left*, ^{27}Al MAS NMR of MK2 (*dash*), sample D (*solid*) and Sample B (*dot*). *Right*, ^{27}Al MAS NMR of MK1 (*dash*), sample K (*solid*) and Sample I (*dot*)

smaller peak attributable to the quartz in the metakaolin is also visible at –107 ppm (Si Q^4 (0Al)).

Again as expected, the unreacted MK1 bands disappear from the ^{1}H-^{29}Si CP MAS NMR spectrum for Sample K, which presents a signal at –86.5 ppm.

The ^{27}Al NMR spectra (Fig. 4) for both MK contain signals indicative of the presence of octahedral, pentahedral and tetrahedral Al [17]. When the samples are activated, bands appear on the spectrum at between 57 and 58 ppm, revealing the existence of tetrahedral Al surrounded by four Si. Samples B and D also contain a small signal attributed to the octahedral Al present in the unreacted MK. The chemical shift in the ^{23}Na is similar in all these samples, denoting the same degree of cation solvation in all cases.

In both types of MK specimens, strength increased with the Na concentration in the activating solutions, peaking at 12 M and declining thereafter. The flexural strength values, in turn, declined with rising doses of activator in the mix. No strength was recorded at any time throughout the duration of the test for the MK2 samples made with the lowest Na concentration.

The flexural strength values for the MK2 paste specimens varied with the Na concentration in keeping with Eq. 1 obtained by polynomial regression fit (Statgraphics), while the variation in MK2 specimen mechanical strength in terms of the volume and concentration—up to 12 M—of the Na in activator is described by expression (2) obtained by multiple regression analysis (Statgraphics):

$$\begin{aligned} R(\text{Mpa}) = & -36.11 + 11.12X_{\text{A}} - 0.799X_{\text{A}}^2 \\ & + 0.0175X_{\text{A}}^3 \quad R^2 = 0.9520 \end{aligned} \tag{1}$$

$$R(\text{Mpa}) = 12.27 + 0.55X_{\text{A}} - 0.16X_{\text{B}} \quad R^2 = 0.7907 \tag{2}$$

Where X_{A} is the Na molar concentration in the activator (mol/l) and X_{B} is the volume of activating solution (ml).

Generally speaking, specimen porosity sank with increasing Na concentration in the activating solutions, reaching the nadir at 12–15 M, after which values sloped upward. Porosity values rose, however, with increasing volume of liquid in the mix.

The findings on insoluble residue are given in Table 1. The values of this parameter declined as the Na concentration in the activating solution and the solution volume grew. Using multiple regression analysis (Statgraphics), the following expressions were found to relate the amount of insoluble residue to Na concentration and volume of liquid:

$$\begin{aligned} \text{MK1}: \ \text{I.R(wt\%)} &= 103.39 - 0.457X_{\text{B}} - 4.994X_{\text{A}} \\ R &= 0.6561 \end{aligned} \tag{3}$$

$$\begin{aligned} \text{MK2}: \ \text{I.R(wt\%)} &= 105.13 - 0.719X_{\text{B}} - 3.2654X_{\text{A}} \\ R &= 0.8174 \end{aligned} \tag{4}$$

Table 2 gives the concentrations of soluble and fixed Na_2O in the pastes, referred to the dry residue (%MK + %Na_2O + %SiO_2) measured in the pastes. Figure 5 shows the sodium fixed in the reaction product versus the initial dose of sodium in the two types of metakaolin. The amount of fixed Na_2O increases with the amount of initial Na_2O up to about 18%wt, but flattens thereafter, remaining more or less constant irrespective of the type of MK.

Two endothermal signals, at 180 and 330 °C, are observed in the DTA/TG for all the samples; and in the MK2 samples an additional endothermal signal,

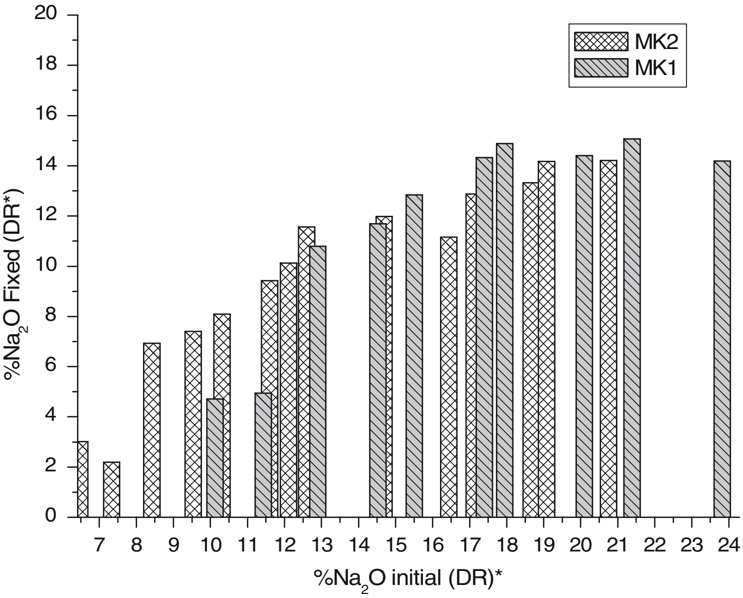

Fig. 5 %wt of fixed Na_2O versus percentage of Na_2O in reactive

attributed to the loss of different types of water, is visible at around 460–500 °C. All the curves also showed a signal at 800 °C attributed to the crystallization of anhydrous sodium aluminosilicate from the hydrated compound formed at lower temperatures. The DTA/TG data for Samples M, D, E and F are given in Table 4.

The Na, Si and Al content in activated pastes D, F and M and in the solid residue remaining after these same pastes were attacked with dilute acid [7], as well as the soluble Na and loss on ignition in activated pastes D, F and M, were measured to determine the composition of the polymer formed during MK1 and MK2 alkali activation. The results of the analyses of the Si, Al and Na content in some of the activated MK pastes and their solid residues after attack with dilute acid are given in Table 5.

The composition of the alkaline polymer formed after alkali activation of metakaolin was determined on the grounds of these analyses, the Na_2O soluble values in samples and the DTA data applying the methodology described in [7]. Table 6 gives the chemical composition of these alkaline polymers and their molar ratios.

Table 5 Si, Al and Na content in pastes and the solid residua in IR test (%wt)

Label		Na_2O	SiO_2	Al_2O_3	L.I.	Soluble Na_2O
Paste	D	10.6	46.6	28.1	10.72	1.98
	F	15.2	42.7	26.1	12.40	3.92
	M	14.2	44.5	23.7	14.77	2.43
Solid residue in IR test	D	0.16	57.42	33.81		
	F	0.21	53.78	32.11		
	M	0.24	60.42	27.95		

Discussion

The composition, structure, microstructure and properties of the polymers formed in the alkali activation of metakaolin depend on the concentration, volume and type of activator used, as well as the characteristics of the metakaolin itself (composition, fineness and so on) [3, 5, 12, 18–20].

The product of metakaolin activation with NaOH solutions is an amorphous cementitious material [3, 6–8] with good mechanical properties [3]. It has been concluded from FTIR, ^{27}Al, ^{29}Si MAS NMR and ^{23}Na

Table 4 Temperature of transformations in DTA curves (°C) and associated TG (%wt)

Label	1st DTA peak T (°C)	TG loss (%wt)	2nd DTA peak T (°C)	TG loss (%wt)	3rd DTA peak T (°C)	TG loss (%wt)	Exo DTA T (°C)	TG (%wt) Total lost
M	180	9.8	330	0.4	–	–	800	14.8
D	180	7.1	340	1	460	1.8	980	11.3
E	190	8.5	340	0.6	500	0.8	840	13.3
F	150	6.2	340	1.2	490	1.7	820	13

Table 6 Oxide composition and molar ratios of the polymers in samples D, F and M (%wt)

Label	% SiO_2	% Al_2O_3	% Na_2O	% H_2O	SiO_2/Al_2O_3	Al_2O_3/Na_2O	SiO_2/Na_2O	SiO_2/H_2O
F	27.87	17.24	11.22	7.4	2.74	0.93	2.56	1.1
D	24.45	15.06	8.55	8.1	2.76	1.07	2.95	0.90
M	34.01	18.84	11.72	10.2	3.06	0.97	2.99	1.00

MAS NMR [7] studies that its three-dimensional structure is a network [Q^4(Al)] consisting in alternating SiO_4 and AlO_4 tetrahedra linked by shared O atoms [7, 12]. The alkali cations in the structure balance the negative charge of the tetrahedrally coordinated Al^{3+} ion. The general formula for the reaction product is $2SiO_2{\cdot}Al_2O_3{\cdot}Na_2O{\cdot}\ 2H_2O$ [7].

When the activator is a NaOH and waterglass mix, the material formed is amorphous and cementitious, but its structure and composition are different from the product formed when NaOH is used alone [12].

Many authors have related the molar composition (SiO_2/Al_2O_3, Na_2O_3/Al_2O_3, Al_2O_3/H_2O) of metakaolin and alkaline solutions mixes to the structure of the polymer obtained, its properties and so on [5, 18–21], but without conducting a chemical analysis of the polymer or determining the degree of reaction or amount of excess alkali. Both the degree of reaction reached in the different pastes and the composition of some of the polymers obtained were found in the present study.

The insoluble residue provides a good measure of the degree of reaction in the samples, for it corresponds to the unreacted MK [3, 7]. It is not a direct measure of the polymer formed, however, for it also contains the zeolite appearing in some of the samples, although given the small amounts of mineral involved, the error is of minor significance.

The IR values for the samples made with the two types of MK show that the degree of reaction increases with the volume and concentration of Na_2O in the activating solution: according to the regression coefficients in Eqs. 3 and 4, the degree of reaction is more sensitive to increases in concentration—rising more sharply—than to increases in volume.

Moreover, the degree of reaction in MK1 is greater than in MK2 samples, due, certainly, to the higher specific surface of the former and the larger volume of activator used. As a result, at any given concentration, the amount of NaOH per gram of metakaolin is much higher in MK1 than MK2 mixes. That higher degree of reaction does not, however, lead to the development of greater mechanical strength, since larger volumes of activating solution induce greater porosity.

The IR (or degree of reaction) varies linearly with the percentage of Na_2O fixed, expressed as a percentage of dry residue. As the degree of formation of the polymer rises (and IR declines), more sodium is fixed as illustrated in Fig. 6 and Eq. 5 obtained by multiple regression analysis (Statgraphics).

$$IR = 85.59 - 4.7878\%\,Na_2O\ \text{fixed}\ R^2 = 0.9890 \tag{5}$$

The values of IR in the MK1 and MK2 samples activated with a sodium silicate + NaOH solution are greater than in analogous samples activated with NaOH alone [3]. In the former in other words, the degree of reaction is smaller and the amount of unreacted metakaolinin greater. This is because the silica in the sodium silicate reacts sooner than the silica in the metakaolin, leaving a larger proportion of unreacted compound (compared to activation with NaOH). Finally, the flexural strength values obtained for NaOH + waterglass-activated MK specimens cured for 2 h at 85 °C were greater than obtained for analogous specimens made with metakaolin activated with NaOH alone [3], despite the lower degree of reaction in the former [3].

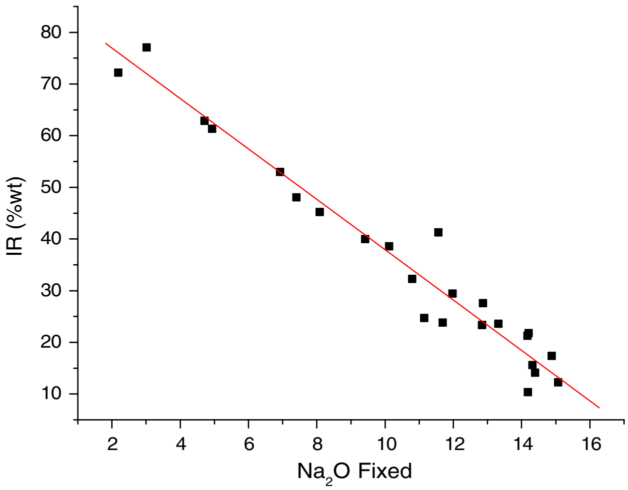

Fig. 6 Variation of paste IR versus Na fixed in the polymer formed

Moreover, pastes D, F and M were analyzed with the aforementioned methodology [7] and the composition of the polymers formed was obtained (Table 6]. The Si/Al ratio was approximately 1.4–1.5, the Al/Na ratio in turn is close to 1, indicating both that the cation is incorporated into the polymer structure, offsetting the entire charge of the Al. The approximate general formula for the polymer formed when metakaolin is activated with sodium silicate + NaOH is: $Na_2O{\cdot}3SiO_2{\cdot}Al_2O_3{\cdot}3H_2O$.

According to the NMR data given in Table 2 and Figs. 3 and 4, the main band on the ^{29}Si MAS NMR spectrum is located at around –90 ppm (from –88.4 to –90.8 ppm); the width of this signal, which is indicative of the existence of different environments for the Si, is due to the overlapping of the band corresponding to the alkaline polymer formed with the band attributed to the unreacted metakaolin in the samples. According to a paper by Duxson et al. [19], the range of frequencies at which the Si Q^4(2Al) and Q^4(3Al) components are found in alkaline polymers is from –95 to –91 ppm and –88 to –85 ppm, respectively; and for samples with a nominal Si/Al value of 1.5, the fraction of Q^4(3Al) silicon is the highest. Rahier et al. [12], in turn, found that as the SiO_2/Na_2O ratio in the activating solution declines, the average amount of Al bound to Si rises. A steady increase in the Al chemical shift is also observed for increasing degree of Al substitution together with a shift of Si–O asymmetric stretching band to lower frequencies in the FTIR spectrum.

Both the position of the band at around 57–58 ppm on the ^{27}Al MAS NMR spectra and the position of the Si–O antisymmetric stretching band in the FTIR spectra at around 1,000 cm^{-1} are compatible with values for Al substitution for Si of about 3 [12]. Moreover, the $^1H^{29}$Si CP MAS NMR signals position at about –87 ppm (Figs. 3, 4) originated by SiOH groups, reveals the existence of Si Q^4 (3Al) in samples. The high concentration of Na and the consequently low SiO_2/Na_2O ratio in the activating solution and the Si/Al ratio measured in the polymers support the hypothesis that the hydrated sodium aluminosilicates formed have a three-dimensional structure in which Q^4 Si (3Al) component predominate.

When a 6-M activator used, the flexural strength values reached by the end of the test time were either undetectable (MK2) or very low (MK1).

As noted in the section on results, flexural strength values rise with declining activator volume and growing Na concentration. The coefficients in Eq. 2 describing the mechanical performance of MK2 specimens show that mechanical strength is affected more by increases in activator concentration than by changes in volume (for variations in the range of values used in this study). Raising the activating solution volume has a dual effect: on the one hand, it is beneficial, prompting a rise in structural Si and Na, while on the other larger volumes of liquid increase porosity, which has an adverse effect on strength.

Moreover, sample flexural strength peaks at an activator concentration of 12 M, turning downward at higher concentrations. This decline in mechanical strength may be due to zeolite crystallization at high concentrations of activator; the presence of this mineral was detected by XRD analysis in all the samples activated with 15-, 18- and 20-M solutions.

Although all the specimens were highly porous, no clear correlation could be found between activator concentration or volume and porosity, or between porosity and mechanical strength.

Conclusions

1. The reaction product of metakaolin activation with sodium silicate + NaOH solutions is an amorphous hydrated sodium aluminosilicate in which a Q^4 Si (3Al) type three-dimensional structure predominated. The alkaline ions in the structure maintain the electrical balance. The general formula obtained for this inorganic polymer was $Na_2O{\cdot}3SiO_2{\cdot}Al_2O_3{\cdot}3H_2O$.
2. The alkali activation of metakaolin with sodium silicate + NaOH solutions produces materials with higher mechanical strength than activation with NaOH alone.
3. The synthesis variables studied (activator concentration and volume) and the specific surface of the initial metakaolin determine the strength of the final product.
   Flexural strength values rise with declining activator volume and higher concentrations of Na. Strength values are affected by increases in activator concentration more than by larger volume.
4. The existence of excess sodium (due to increases in activator concentration) leads to sodalite or faujasite crystallization, which has an adverse effect on strength development.

Acknowledgements The authors are grateful Dr. Jesús Sanz and Dr. Mª Isabel Sobrados for their help in the interpretation of NMR. They also thank to CICYT for the funding received from project MAT2003-08343. Dr Sagrario Martínez-Ramírez participated in this research under a Ramon y Cajal contract awarded by the Ministry of Science and Technology and co-funded by the European Social Fund.

References

1. Davidovits J (1982) Mineral polymers and methods of making them. US Patent No 4472 199
2. Krivenko P (1997) Alkaline cements: terminology, classification, aspects of durability. In: Proceeding of the Tenth International Congress on Chemistry of Cement, Göteborg, vol 4, p 4iv046
3. Granizo ML, Blanco MT, Puertas F, Palomo A (1997) Alkaline activation of metacaolin: influence of synthesis parameters. In: Proceeding of the Tenth International Congress on Chemistry of Cement, Göteborg, vol 3, p 3ii113
4. Granizo ML, Blanco-Varela MT, Palomo A (2000) J Mater Sci 35(24):6309
5. Barbosa VFF, MacKenzie KJD, Thaumaturgo C (2000) Int J Inorg Mater 2(4):309
6. Singh PS, Trigg M, Burgar I, Bastow T (2005) Sci Eng A 396:392
7. Granizo ML, Alonso S, Blanco-Varela MT, Palomo A (2002) J Am Ceram Soc 85(1):225
8. Granizo ML, Blanco-Varela MT (1998) J Therm Anal 52:957
9. Brindley GW, Wardle R (1970) Am Mineral 55:1259
10. Wardle R, Brindley GW (1972) Am Mineral 57:732
11. Palomo A, Glasser FP (1992) Br Ceram Trans J 91(4):107
12. Rahier H, Simons W, van Mele B, Biesemans M (1997) J Mater Sci 32(9):2237
13. Percival HJ, Duncan JF, Foster PK (1974) J Am Ceram Soc 57(2):57
14. Palomo A, Blanco-Varela MT, Granizo ML, Puertas F, Vazquez T, Grutzeck MW (1999) Cem Concr Res 29:997
15. Erdemoğlu M, Erdemoğlu S, Sayılkan F, Akarsu M, Ş ener Ş , Sayılkan H (2004) Appl Clay Sci 27(1–2):41
16. Singh PS, Trigg M, Burgar I, Bastow T (2002) 27Al and 29Si MAS-NMR study of aluminosilicate polymer formation at room temperature. Geopolymers 2002. Turn Potential into Profit: Melbourne, Australia
17. Madani A, Aznar A, Sanz J, Serratosa JM (1990) J Phys Chem 94:760
18. Rahier H, Denayer JF, van Mele B (2003) J Mater Sci 38(1):3131
19. Duxson P, Provis JL, Lukey GC, Separovic F, van Deventer JSJ (2005) Langmuir 21(7):3028
20. Steveson M, Sagoe-Crentsil K (2005) J Mater Sci 40:2023
21. Duxson PL, Provis JL, Lukey GC, Mallicoat SW, Kriven WM, van Deventer JSJ (2005) Colloids Surf 26:47